NATIONAL ADVISORY COMMITTEE
FOR AERONAUTICS

TECHNICAL NOTE

No. 1708

THEORETICAL CHARACTERISTICS IN SUPERSONIC FLOW OF

CONSTANT-CHORD PARTIAL-SPAN CONTROL

SURFACES ON RECTANGULAR WINGS

HAVING FINITE THICKNESS

By Warren A. Tucker and Robert L. Nelson

Langley Aeronautical Laboratory
Langley Field, Va.

Washington

September 1948

NATIONAL ADVISORY COMMITTEE FOR AERONAUTICS

TECHNICAL NOTE NO. 1708

THEORETICAL CHARACTERISTICS IN SUPERSONIC FLOW OF

CONSTANT-CHORD PARTIAL-SPAN CONTROL

SURFACES ON RECTANGULAR WINGS

HAVING FINITE THICKNESS

By Warren A. Tucker and Robert L. Nelson

SUMMARY

The Busemann third-order approximation for two-dimensional isentropic
flow was used in suitable conjunction with three-dimensional solutions
found by the linearized theory to determine analytically, for small angles
of attack and control deflections, the control-surface characteristics of
partial-span constant-chord flaps on rectangular wings having finite
thickness.

The control surfaces were considered to extend either outboard from
the center line or inboard from the wing tip. Although only flat-sided
control surfaces were treated, the general method can be extended to
control surfaces having curved sides.

Equations were found for the lift coefficient, rolling-moment coef-
ficient, and hinge-moment coefficient due to control deflection, and for
the pitching-moment coefficient due to flap lift. The effect of thickness
was shown to be given by a single factor.

INTRODUCTION

Much work has been done on three-dimensional control-surface char-
acteristics by using the linearized equations of supersonic flow.
(See references 1 to 4.) In reference 5, two-dimensional control-
surface characteristics were found by the use of more exact methods.
Although references 1 to 4 characteristically show no effect of airfoil
thickness, reference 5 shows that the effect of thickness influenced
the control-surface characteristics when higher-order terms were taken
into account. In the present paper, the Busemann third-order approxi-
mation for two-dimensional isentropic flow is used together with three-
dimensional solutions found by use of the linearized theory to determine
the characteristics of partial-span, constant-chord control surfaces on
rectangular wings having finite thickness. The method used to combine
the two types of solutions consists of multiplying the pressures found
from the linearized theory by a factor such that in a region of two-
dimensional flow the pressure is made equal to that found from the

Busemann third—order approximation. Simple expressions are found for the lift coefficient, rolling—moment coefficient, and hinge—moment coefficient due to control deflection and for the pitching—moment coefficient due to flap lift.

The results are subject to all the limitations of the third—order approximation. Some discussion of these limitations is given in reference 6. Additional errors are introduced by the combination of two theories having different degrees of approximation. Boundary—layer effects have been neglected.

SYMBOLS

A wing aspect ratio $\left(\dfrac{b}{c}\right)$

b wing span

b_f flap span

c wing chord

$\overline{c}$ wing mean aerodynamic chord (c)

c_f flap chord

$\overline{c}_f$ flap root—mean—square chord (c_f)

$$C_1 \equiv \frac{2}{\sqrt{M^2 - 1}} \equiv \frac{2}{\beta}$$

$$C_2 \equiv \frac{(\gamma + 1)M^4 - 4(M^2 - 1)}{2(M^2 - 1)^2}$$

$$C_3 \equiv \frac{1}{6(M^2 - 1)^{7/2}}\left[(\gamma + 1)M^8 + \left(2\gamma^2 - 7\gamma - 5\right)M^6 + 10(\gamma + 1)M^4 - 12M^2 + 8\right]$$

C_L lift coefficient $\left(\dfrac{L}{qS}\right)$

C_m pitching—moment coefficient $\left(\dfrac{M}{qS\overline{c}}\right)$

C_l rolling-moment coefficient $\left(\dfrac{l}{qSb}\right)$

C_h hinge-moment coefficient $\left(\dfrac{H}{qb_f \dfrac{\overline{c}_f{}^2}{2}}\right)$

C_p lifting-pressure coefficient $\left(\dfrac{P}{q}\right)$

H hinge moment of one flap

H_1 hinge moment over inboard corner of one flap

H_2 hinge moment over two-dimensional part of one flap

H_3 hinge moment over outboard corner of one flap

L lift of two flaps

l rolling moment of two flaps

M free-stream Mach number; pitching moment of two flaps about midchord of wing

P lifting pressure

p local static pressure

p_0 free-stream static pressure

q free-stream dynamic pressure $\left(\dfrac{\rho V^2}{2}\right)$

S wing area (bc)

V free-stream velocity

x,y Cartesian coordinates parallel and normal, respectively, to free-stream direction

$\beta \equiv \sqrt{M^2 - 1}$

γ ratio of specific heat at constant pressure to specific heat at constant volume (1.40 for air)

δ angle of flap deflection

θ angle of surface with respect to free stream, positive when
         direction of flow is toward surface

$\nu \equiv \dfrac{\beta y}{x}$

ρ free-stream density

$\emptyset$ trailing-edge angle

Subscripts:

δ partial derivative of coefficient with respect to δ, taken
         at $\delta = 0$ $\left(\text{example: } C_{L_\delta} \equiv \left(\dfrac{\partial C_L}{\partial \delta}\right)_{\delta=0}\right)$

C_L partial derivative of coefficient with respect to C_L, taken
         at $\delta = 0$

∞ two-dimensional

u   upper surface

l lower surface

av   average value

   All angles are in radians, unless otherwise specified.

ANALYSIS

   The control-surface configurations investigated are shown in figure 1.
The only limitations on the airfoil section are that the flap must have
flat sides, the section must be symmetrical about the chord line, and the
leading-edge angle must be small enough so that the shock wave is attached.
Because the pressures over certain parts of the inboard and outboard flaps
are identical, both cases are treated in this paper.

   The angle of attack and the control deflection are assumed to be
small, and the chordwise gaps between the wing and the flap are assumed
to be sealed. The additional assumption is made that the effects of
angle of attack and control deflection are mutually independent and can
be superposed. Although this assumption is not strictly true, it is a
good engineering approximation for the small angles considered.

   The control-surface characteristics to be found are as follows:

   C_{L_δ} lift coefficient due to flap deflection

C_{l_δ} rolling-moment coefficient due to flap deflection

C_{h_δ} hinge-moment coefficient due to flap deflection

$C_{m_{C_L}}$ pitching-moment coefficient (about the midchord) due to flap lift

The only information required to find these coefficients is the pressure distribution due to flap deflection, which, within the limitations of the present analysis, is independent of the airfoil section so long as the flap is flat sided. To find the hinge-moment coefficient due to angle of attack would require a knowledge of the pressure distribution due to angle of attack, which would be a function of the airfoil section. Even for a particular airfoil section, this pressure distribution cannot be found to the same degree of approximation as the pressure distribution due to flap deflection by using the assumptions of the present analysis. In order to preserve the generality of the analysis, the equations for this coefficient, therefore, have not been derived.

Pressure distributions.— The aforementioned coefficients are easily determined if the pressure distribution due to flap deflection is known. In the region between the Mach cones from the corners of the flap, the flow is two-dimensional. Then, according to the Busemann third-order approximation to isentropic flow,

$$\frac{p - p_0}{q} = C_1\theta + C_2\theta^2 + C_3\theta^3$$

If the angles are considered positive for compression and negative for expansion, then from figure 1(c)

$$\theta_l = \left(\delta - \frac{\phi}{2}\right)$$

$$\theta_u = -\left(\delta + \frac{\phi}{2}\right)$$

Then,

$$\frac{p_l - p_0}{q} = C_1\left(\delta - \frac{\phi}{2}\right) + C_2\left(\delta^2 - \phi\delta + \frac{\phi^2}{4}\right) + C_3\left(\delta^3 - \frac{3\phi\delta^2}{2} + \frac{3}{4}\phi^2\delta - \frac{\phi^3}{8}\right)$$

$$\frac{p_u - p_0}{q} = -C_1\left(\delta + \frac{\phi}{2}\right) + C_2\left(\delta^2 + \phi\delta + \frac{\phi^2}{4}\right) - C_3\left(\delta^3 + \frac{3}{2}\phi\delta^2 + \frac{3}{4}\phi^2\delta + \frac{\phi^3}{8}\right)$$

The net lifting-pressure coefficient is then

$$C_p = \frac{P}{q} = \frac{p_l - p_0}{q} - \frac{p_u - p_0}{q} = 2C_1\delta - 2C_2\delta\emptyset + 2C_3\delta^3 + \frac{3}{2}C_3\emptyset^2\delta$$

$$= 2\delta\left(C_1 - C_2\emptyset + \frac{3}{4}C_3\emptyset^2\right) + 2C_3\delta^3$$

Within the Mach cones from the corners of the flaps, the pressure varia-
tions have been previously determined by use of the linear theory (refer-
ences 4 and 7). In the present analysis the shapes of the pressure
distribution inside the tip Mach cones are assumed to be identical to
those found by use of the linear theory, but the ordinates are multiplied
by a constant factor such that the value of the pressure at the inner
limit of the Mach cone equals the two-dimensional pressure found by use of
the third-order approximation. The pressure distributions over both
inboard and outboard flaps are shown in figure 2, together with the equa-
tions for the pressure variation.

Derivation of control-surface characteristics.— With the pressure
distributions known, expressions for the control-surface characteristics
may be obtained by following the procedure of reference 3. For the sake
of brevity, the derivation of only one of these characteristics, C_{h_δ} for
outboard flaps, is given.

Over the two-dimensional part of a flap the lifting-pressure coeffi-
cient is given by

$$C_p = 2\delta\left(C_1 - C_2\emptyset + \frac{3}{4}C_3\emptyset^2\right) + 2C_3\delta^3$$

and

$$\frac{\partial C_p}{\partial \delta} = 2\left(C_1 - C_2\emptyset + \frac{3}{4}C_3\emptyset^2\right) + 6C_3\delta^2$$

At $\delta = 0$,

$$\frac{\partial C_p}{\partial \delta} = 2\left(C_1 - C_2\emptyset + \frac{3}{4}C_3\emptyset^2\right)$$

Over the two-dimensional part of one flap,

$$\left(\frac{\partial \frac{H_2}{q}}{\partial \delta} \right)_{\delta=0} = -2\left(C_1 - C_2\phi + \frac{3}{4} C_3\phi^2 \right) \left(\frac{c_f}{2} \frac{b_f}{2} c_f - \frac{2}{3} c_f \frac{c_f^2}{\beta} \right)$$

$$= -\left(C_1 - C_2\phi + \frac{3}{4} C_3\phi^2 \right) \left(\frac{b_f c_f^2}{2} - \frac{4}{3} \frac{c_f^3}{\beta} \right)$$

Over the inboard corner of the flap, the average lifting-pressure coefficient is given by

$$C_{p_{av}} = \frac{C_{p_\infty}}{2} \int_0^1 \left(1 + \frac{2}{\pi} \sin^{-1} \nu \right) d\nu$$

$$= \frac{C_{p_\infty}}{2} \left[\nu + \frac{2}{\pi} \nu \sin^{-1} \nu + \frac{2}{\pi} \sqrt{1 - \nu^2} \right]_0^1$$

$$= \frac{C_{p_\infty}}{2} \left(1 + 1 - \frac{2}{\pi} \right)$$

$$C_{p_{av}} = C_{p_\infty} \left(1 - \frac{1}{\pi} \right)$$

Then, because the flow is conical, the center of pressure in this region is at $\frac{2}{3} c_f$ and

$$\left(\frac{\partial \frac{H_1}{q}}{\partial \delta} \right)_{\delta=0} = -2\left(C_1 - C_2\phi + \frac{3}{4} C_3\phi^2 \right) \left(1 - \frac{1}{\pi} \right) \frac{2}{3} c_f \frac{c_f^2}{2\beta}$$

$$= -\left(C_1 - C_2\phi + \frac{3}{4} C_3\phi^2 \right) \left(1 - \frac{1}{\pi} \right) \frac{2 c_f^3}{3\beta}$$

Over the outboard corner of the flap, the average pressure is one-half the two-dimensional value. Then, because the flow in this region is also conical,

$$\left(\frac{\partial \frac{H_3}{q}}{\partial \delta}\right)_{\delta=0} = -\left(c_1 - c_2\phi + \frac{3}{4}c_3\phi^2\right)\frac{2}{3}\,c_f\,\frac{c_f^2}{2\beta}$$

$$= -\left(c_1 - c_2\phi + \frac{3}{4}c_3\phi^2\right)\frac{c_f^3}{3\beta}$$

Over the entire flap,

$$\left(\frac{\partial \frac{H}{q}}{\partial \delta}\right)_{\delta=0} = -\left(c_1 - c_2\phi + \frac{3}{4}c_3\phi^2\right)\left(\frac{b_f c_f^2}{2} - \frac{4}{3}\frac{c_f^3}{\beta} + \frac{2c_f^3}{3\beta} - \frac{2c_f^3}{3\pi\beta} + \frac{c_f^3}{3\beta}\right)$$

$$= -\left(c_1 - c_2\phi + \frac{3}{4}c_3\phi^2\right)\left(\frac{b_f c_f^2}{2} - \frac{1}{3}\frac{c_f^3}{\beta} - \frac{2c_f^3}{3\pi\beta}\right)$$

$$= -\left(c_1 - c_2\phi + \frac{3}{4}c_3\phi^2\right)\left(\frac{b_f c_f^2}{2} - \frac{\pi+2}{3\pi\beta}\,c_f^3\right)$$

Dividing by $b_f c_f^2/2$ gives the coefficient

$$c_{h_\delta} = -\left(c_1 - c_2\phi + \frac{3}{4}c_3\phi^2\right)\left(1 - 2\,\frac{\pi+2}{3\pi\beta}\,\frac{c_f}{b_f}\right)$$

Since

$$\frac{c_f}{b_f} = \frac{c_f}{c}\frac{c}{b}\frac{b}{b_f} = \frac{c_f/c}{Ab_f/b}$$

$$c_{h_\delta} = -\left(c_1 - c_2\phi + \frac{3}{4}c_3\phi^2\right)\left(1 - 2\,\frac{\pi+2}{3\pi\beta A}\,\frac{c_f/c}{b_f/b}\right)$$

or, since $C_1 = \dfrac{2}{\beta}$,

$$C_{h_\delta} = -\frac{2}{\beta}\left(1 - \frac{C_2}{C_1}\phi + \frac{3}{4}\frac{C_3}{C_1}\phi^2\right)\left(1 - \frac{2}{3\beta A}\frac{\pi + 2}{\pi}\frac{c_f/c}{b_f/b}\right)$$

DISCUSSION AND CONCLUDING REMARKS

The final equations, which were derived in a fashion similar to that of the preceding example, are presented in tables I and II. Included in these tables is the range of applicability for each equation; the limits were determined by the method described in appendix C of reference 4. Note that the original equations for C_{h_δ} have been extended to include a wider range of ratios of flap span to wing span. These extensions were derived in a manner similar to that used in appendix D of reference 4. As an illustration of the application of the equations, control-surface characteristics calculated for two particular configurations are shown in figure 3.

An error has been found recently in the value of C_3 as originally given by Busemann. (See references 8 and 9.) The value of C_3 used in the present paper is that given in references 8 and 9. Values of C_1, C_2, and C_3 are given in table III.

Each equation $\left(\text{except those equations for } C_{m_{C_L}}\right)$ contains the factor $\left(1 - \dfrac{C_2}{C_1}\phi + \dfrac{3}{4}\dfrac{C_3}{C_1}\phi^2\right)$, which can be regarded as a reduction factor representing the effect of the finite thickness. When the trailing-edge angle ϕ is zero, this factor is unity, and the equations become those given by the linearized theory. When ϕ is greater than zero, the factor is less than unity, which shows that the effect of the finite thickness is to reduce the absolute magnitude of all the coefficients $\left(\text{except } C_{m_{C_L}}\right)$. Curves of this reduction factor plotted against trailing-edge angle for various Mach numbers are given in figure 4. The stopping point of the curve for $M = 1.3$ was obtained by comparison of this curve with calculations for a double-wedge airfoil with flap made by the exact method of reference 10, the curve given in figure 4 being stopped when a 10-percent difference between the two curves was reached. For the other values of Mach number noted in figure 4, the curves given practically coincided with the exact curves for the entire plotted range of trailing-edge angle.

The recommended range of application (also obtained by comparison
with calculations obtained by use of the method of reference 10) is given
in figure 5. The line of possible flow separation at $\emptyset = 30^\circ$ is quite
arbitrary and is intended to serve as a warning against injudicious use
of the equations rather than as a definite boundary.

Langley Aeronautical Laboratory
    National Advisory Committee for Aeronautics
        Langley Field, Va., May 13, 1948

REFERENCES

1. Lagerstrom, P. A., and Graham, Martha E.: Linearized Theory of Super-
      sonic Control Surfaces. Rep. No. SM–13060, Douglas Aircraft Co.,
      Inc., July 24, 1947.

2. Tucker, Warren A.: Characteristics of Thin Triangular Wings with
      Triangular–Tip Control Surfaces at Supersonic Speeds with Mach Lines
      behind the Leading Edge. NACA TN No. 1600, 1948.

3. Tucker, Warren A.: Characteristics of Thin Triangular Wings with
      Constant–Chord Full–Span Control Surfaces at Supersonic Speeds.
      NACA TN No. 1601, 1948.

4. Tucker, Warren A., and Nelson, Robert L.: Characteristics of Thin
      Triangular Wings with Constant–Chord Partial–Span Control Surfaces
      at Supersonic Speeds. NACA TN No. 1660, 1948.

5. Ivey, H. Reese: Notes on the Theoretical Characteristics of Two–
      Dimensional Supersonic Airfoils. NACA TN No. 1179, 1947.

6. Laitone, Edmund V.: Exact and Approximate Solutions of Two–Dimensional
      Oblique Shock Flow. Jour. Aero. Sci., vol. 14, no. 1, Jan. 1947,
      pp. 25–41.

7. Busemann, Adolf: Infinitesimal Conical Supersonic Flow. NACA TM
      No. 1100, 1947.

8. Puckett, Allen E., and Li, Ting Yi: Letter to the Editor. Jour. Aero.
      Sci., vol. 14, no. 6, June 1947, p. 336.

9. Chang, Chieh–Chien: Letter to the Editor. Jour. Aero. Sci., vol. 14,
      no. 8, Aug. 1947, p. 456.

10. Ivey, H. Reese, Stickle, George W., and Schuettler, Alberta: Charts
      for Determining the Characteristics of Sharp–Nose Airfoils in Two–
      Dimensional Flow at Supersonic Speeds. NACA TN No. 1143, 1947.

TABLE I

OUTBOARD FLAPS

Quantity	Equation number	Equation	Range	
			$\left(b_f/b\right)_{min}$	$\left(b_f/b\right)_{max}$
c_{L_δ}	1	$c_{L_\delta} = \dfrac{2}{\beta}\left(1 - \dfrac{c_2}{c_1}\phi + \dfrac{3}{4}\dfrac{c_3}{c_1}\phi^2\right)\left[2\dfrac{b_f}{b}\dfrac{c_f}{c} - \dfrac{1}{\beta A}\left(\dfrac{c_f}{c}\right)^2\right]$	$\dfrac{2}{\beta A}\dfrac{c_f}{c}$	[a] 1
c_{l_δ}	2	$c_{l_\delta} = \dfrac{1}{\beta}\left(1 - \dfrac{c_2}{c_1}\phi + \dfrac{3}{4}\dfrac{c_3}{c_1}\phi^2\right)\left\{\left[2\dfrac{b_f}{b} - \left(\dfrac{b_f}{b}\right)^2\right]\dfrac{c_f}{c} - \dfrac{1}{\beta A}\left(\dfrac{c_f}{c}\right)^2 - \dfrac{1}{6\beta^2 A^2}\left(\dfrac{c_f}{c}\right)^3\right\}$	$\dfrac{2}{\beta A}\dfrac{c_f}{c}$	[b] 1
$c_{m_{C_L}}$	3	$c_{m_{C_L}} = -\dfrac{1 - \dfrac{c_f}{c} - \dfrac{1}{6\beta A}\left(3 - 2\dfrac{c_f}{c}\right)\dfrac{c_f/c}{b_f/b}}{2 - \dfrac{1}{\beta A}\dfrac{c_f/c}{b_f/b}}$	$\dfrac{2}{\beta A}\dfrac{c_f}{c}$	[a] 1
c_{h_δ}	4	$c_{h_\delta} = -\dfrac{2}{\beta}\left(1 - \dfrac{c_2}{c_1}\phi + \dfrac{3}{4}\dfrac{c_3}{c_1}\phi^2\right)\left(1 - \dfrac{2}{3\beta A}\dfrac{\pi+2}{\pi}\dfrac{c_f/c}{b_f/b}\right)$	$\dfrac{2}{\beta A}\dfrac{c_f}{c}$	$1 - \dfrac{1}{\beta A}\dfrac{c_f}{c}$
c_{h_δ}	5	$c_{h_\delta} = -\dfrac{2}{\beta}\left(1 - \dfrac{c_2}{c_1}\phi + \dfrac{3}{4}\dfrac{c_3}{c_1}\phi^2\right)\left[1 - \dfrac{2}{3\beta A}\dfrac{\pi+2}{\pi}\dfrac{c_f/c}{b_f/b}\right.$ $+ \dfrac{4\left(\dfrac{c_f}{c}\right)^2 + 2\beta^2 A^2\left(1 - \dfrac{b_f}{b}\right)^2}{3\pi\beta A\dfrac{b_f}{b}\dfrac{c_f}{c}}\sqrt{1 - \dfrac{\beta^2 A^2\left(1 - \dfrac{b_f}{b}\right)^2}{\left(\dfrac{c_f}{c}\right)^2}}$ $\left.- \dfrac{2}{\pi}\dfrac{1 - \dfrac{b_f}{b}}{b_f/b}\cos^{-1}\dfrac{\beta A\left(1 - \dfrac{b_f}{b}\right)}{c_f/c}\right]$	$1 - \dfrac{1}{\beta A}\dfrac{c_f}{c}$	[a] 1

NACA

[a] When $\dfrac{b_f}{b} = 1$, $\left(\dfrac{c_f}{c}\right)_{max} = \beta A$.

[b] When $\dfrac{b_f}{b} = 1$, $\left(\dfrac{c_f}{c}\right)_{max} = \dfrac{\beta A}{2}$.

TABLE II

INBOARD FLAPS

| Quantity	Equation number	Equation	Range	
			$(b_f/b)_{min}$	$(b_f/b)_{max}$
$c_{L\delta}$	6	$c_{L\delta} = \dfrac{2}{\beta}\left(1 - \dfrac{c_2}{c_1}\phi + \dfrac{3}{4}\dfrac{c_3}{c_1}\phi^2\right) 2\dfrac{b_f}{b}\dfrac{c_f}{c}$	[a] 0	$1 - \dfrac{2}{\beta A}\dfrac{c_f}{c}$
$c_{l\delta}$	7	$c_{l\delta} = \dfrac{1}{\beta}\left(1 - \dfrac{c_2}{c_1}\phi + \dfrac{3}{4}\dfrac{c_3}{c_1}\phi^2\right)\left(\dfrac{b_f}{b}\right)^2\dfrac{c_f}{c}$	[a] 0	$1 - \dfrac{2}{\beta A}\dfrac{c_f}{c}$
$c_{m_{C_L}}$	8	$c_{m_{C_L}} = -\dfrac{1}{2}\left(1 - \dfrac{c_f}{c}\right)$	[a] 0	$1 - \dfrac{2}{\beta A}\dfrac{c_f}{c}$
$c_{h\delta}$	9	$c_{h\delta} = -\dfrac{2}{\beta}\left(1 - \dfrac{c_2}{c_1}\phi + \dfrac{3}{4}\dfrac{c_3}{c_1}\phi^2\right)\left(1 - \dfrac{4}{3\pi\beta A}\dfrac{c_f/c}{b_f/b}\right)$	$\dfrac{1}{\beta A}\dfrac{c_f}{c}$	$1 - \dfrac{1}{\beta A}\dfrac{c_f}{c}$
$c_{h\delta}$	10	$c_{h\delta} = -\dfrac{4}{\pi\beta}\left(1 - \dfrac{c_2}{c_1}\phi + \dfrac{3}{4}\dfrac{c_3}{c_1}\phi^2\right)\left[\sin^{-1}\dfrac{\beta A b_f/b}{c_f/c} - \dfrac{2c_f/c}{3\beta A b_f/b}\right.$ $\left. + \dfrac{2\left(\dfrac{c_f}{c}\right)^2 + \beta^2 A^2\left(\dfrac{b_f}{b}\right)^2}{3\beta A \dfrac{b_f}{b}\dfrac{c_f}{c}}\sqrt{1 - \dfrac{\beta^2 A^2\left(\dfrac{b_f}{b}\right)^2}{\left(\dfrac{c_f}{c}\right)^2}}\right]$	[a] 0	$\dfrac{1}{\beta A}\dfrac{c_f}{c}$

NACA

[a] When $\dfrac{b_f}{b} = 0$, $\left(\dfrac{c_f}{c}\right)_{max} = \dfrac{\beta A}{2}$.

TABLE III

VALUES OF C_1, C_2, AND C_3

M	C_1	C_2	C_3
1.1	4.364	30.32	867.
1.2	3.015	8.307	53.8
1.3	2.408	4.300	14.4
1.4	2.041	2.919	5.80
1.5	1.789	2.288	3.06
1.6	1.601	1.950	1.97
2.0	1.155	1.467	.927
3.0	.7071	1.269	1.13
4.0	.5164	1.232	1.51

V

(a) Outboard flaps.

V

(b) Inboard flaps.

Section optional

V

δ

ϕ
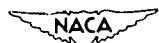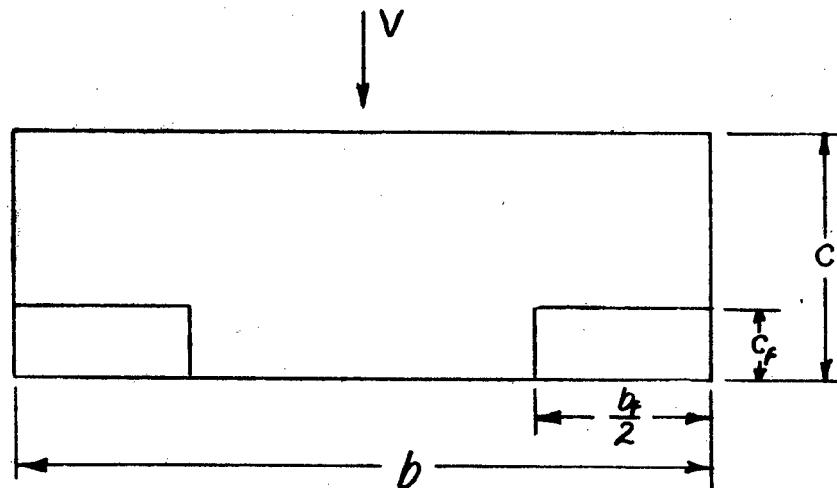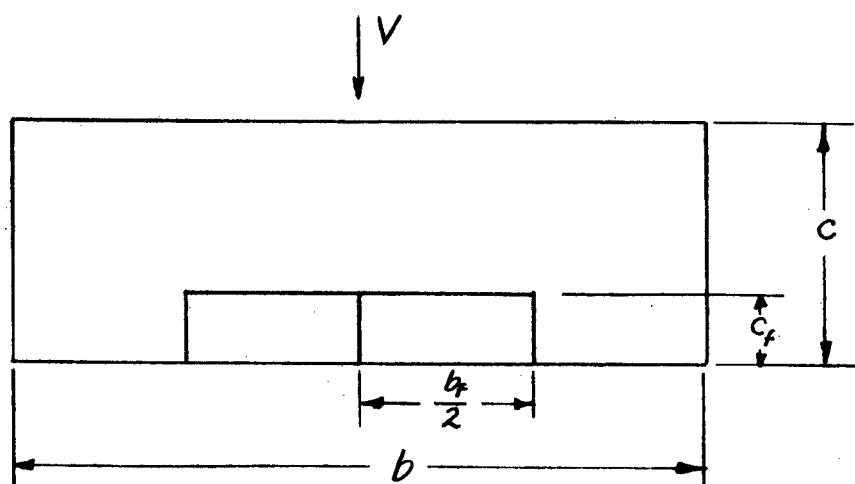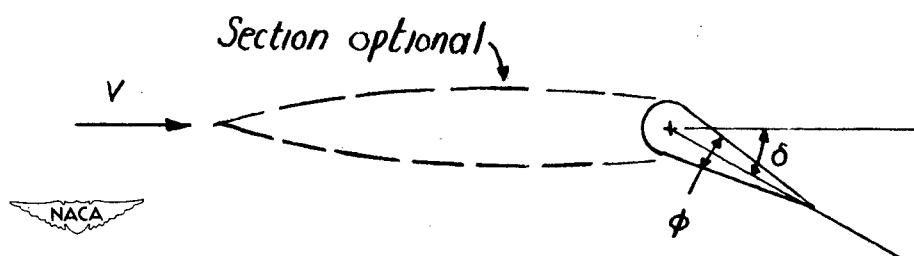
NACA

(c) Section through flap.

Figure 1.- Control-surface configurations investigated.

Pressure on section A-A

$$C_{p_1} = C_{p_3} = C_{p\infty}\left(\frac{1}{2} + \frac{\sin^{-1}\nu}{\pi}\right)$$

$$C_{p_2} = C_{p\infty}$$
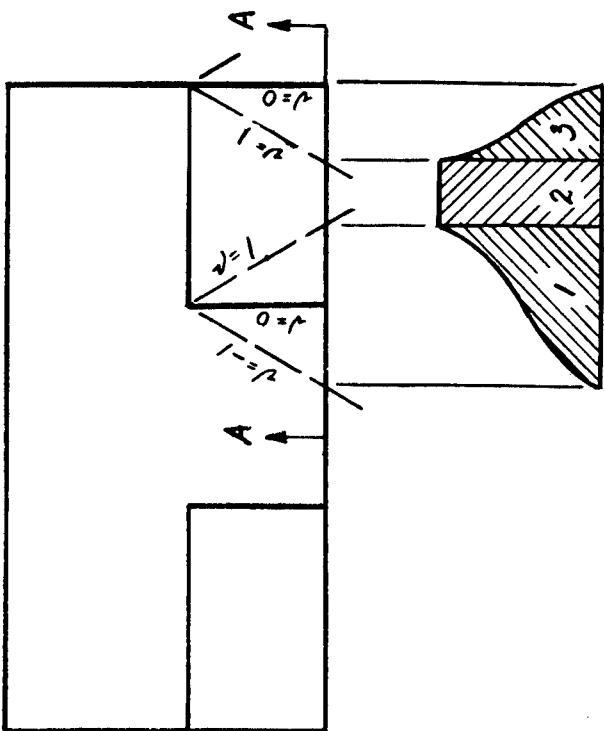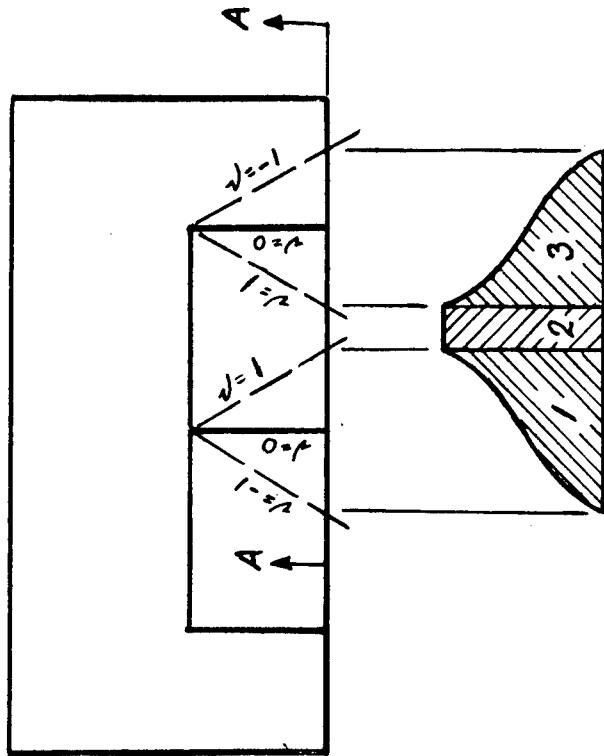
(b)　Inboard flap.

Pressure on section A-A

$$C_{p_1} = C_{p\infty}\left(\frac{1}{2} + \frac{\sin^{-1}\nu}{\pi}\right)$$

$$C_{p_2} = C_{p\infty}$$

$$C_{p_3} = C_{p\infty}\frac{2}{\pi}\sin^{-1}\sqrt{\nu}$$

(a)　Outboard flap.

Figure 2.-　Pressure distributions due to flap deflection.
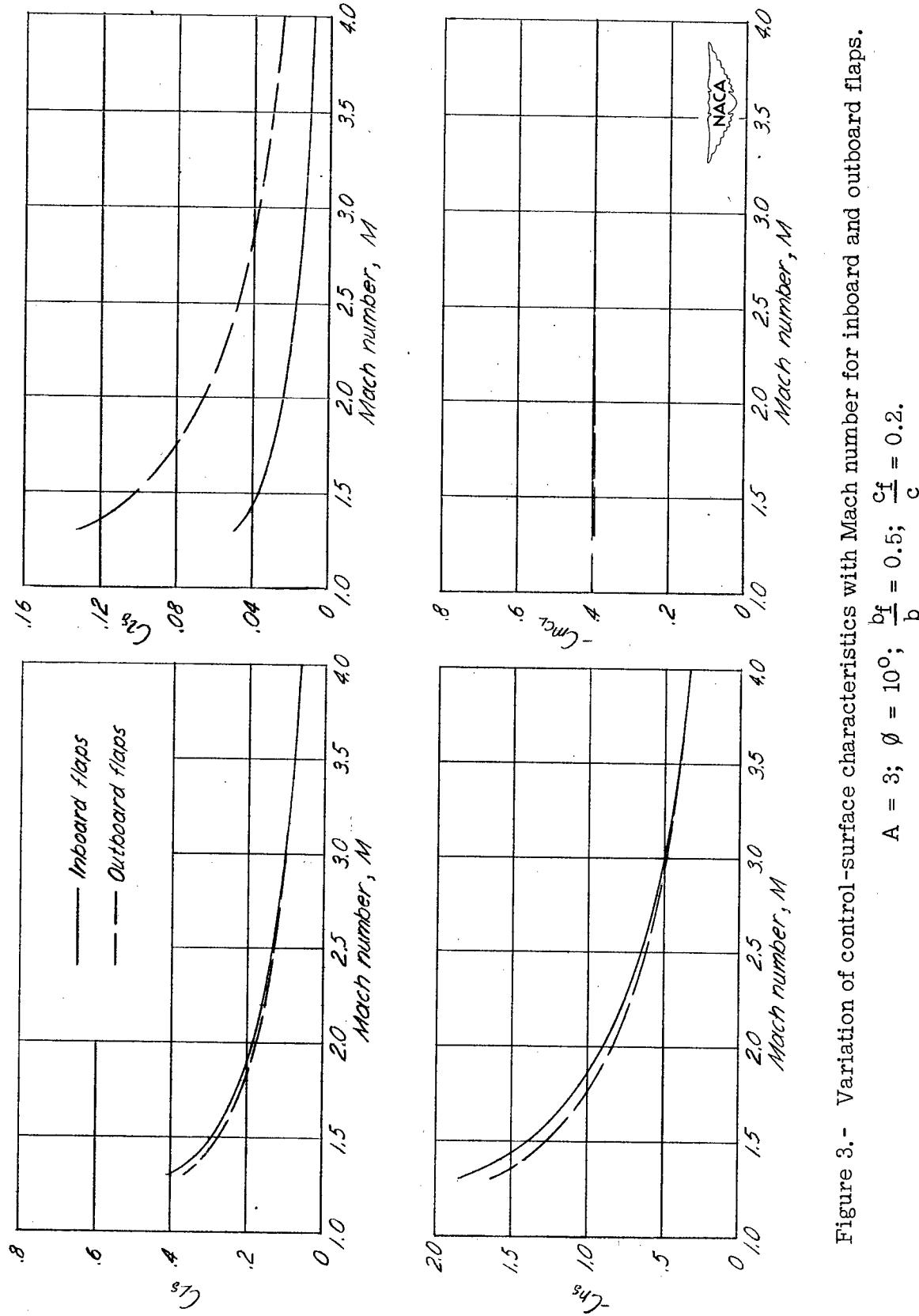
Figure 3.- Variation of control-surface characteristics with Mach number for inboard and outboard flaps.

$$A = 3; \quad \phi = 10°; \quad \frac{b_f}{b} = 0.5; \quad \frac{c_f}{c} = 0.2.$$

The vertical axis is labeled $1 - \dfrac{C_2}{C_1}\,\phi + \dfrac{3}{4}\dfrac{C_3}{C_1}\,\phi^2$

The horizontal axis is labeled ϕ, deg
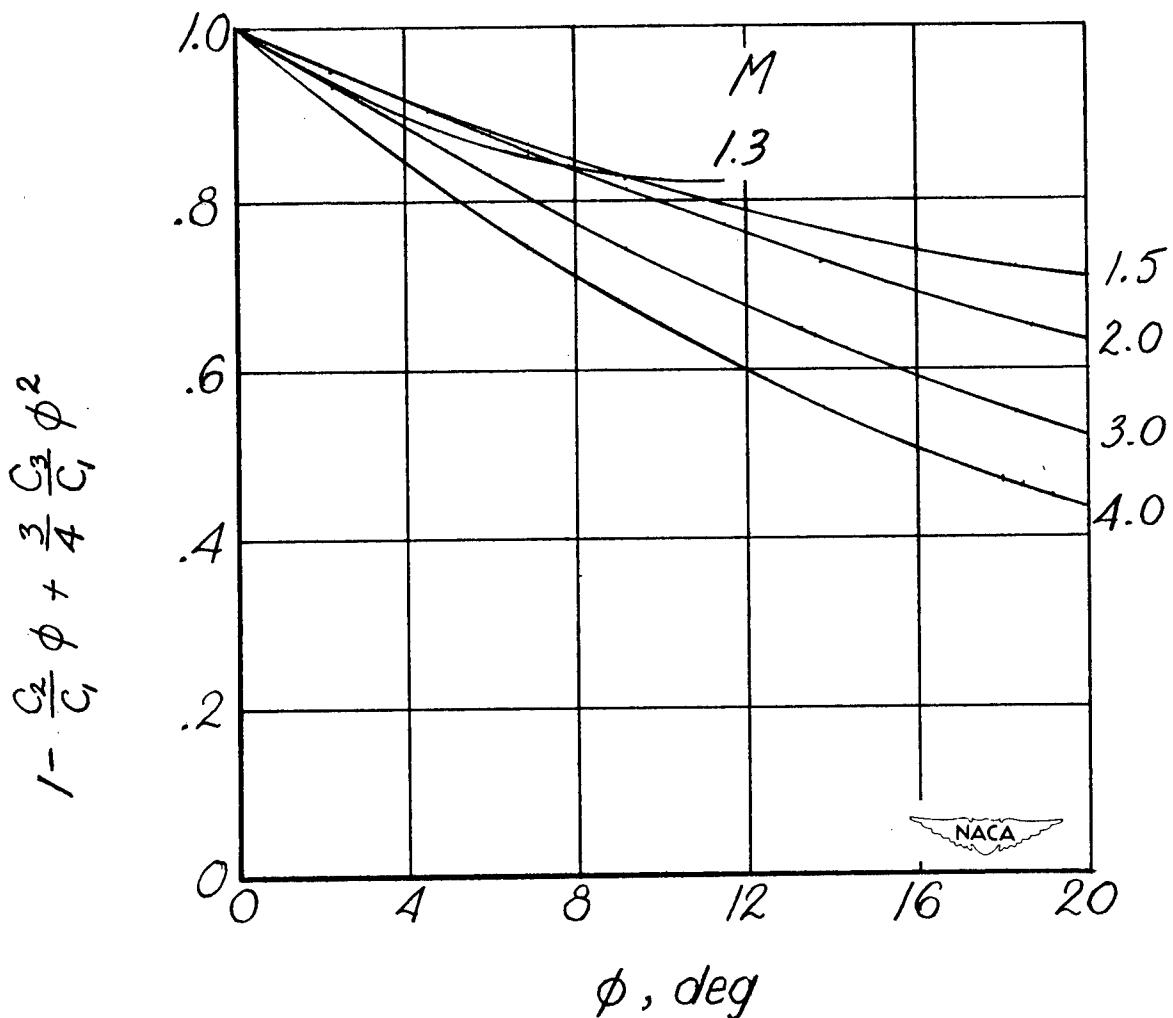
Figure 4.- Thickness reduction factor.
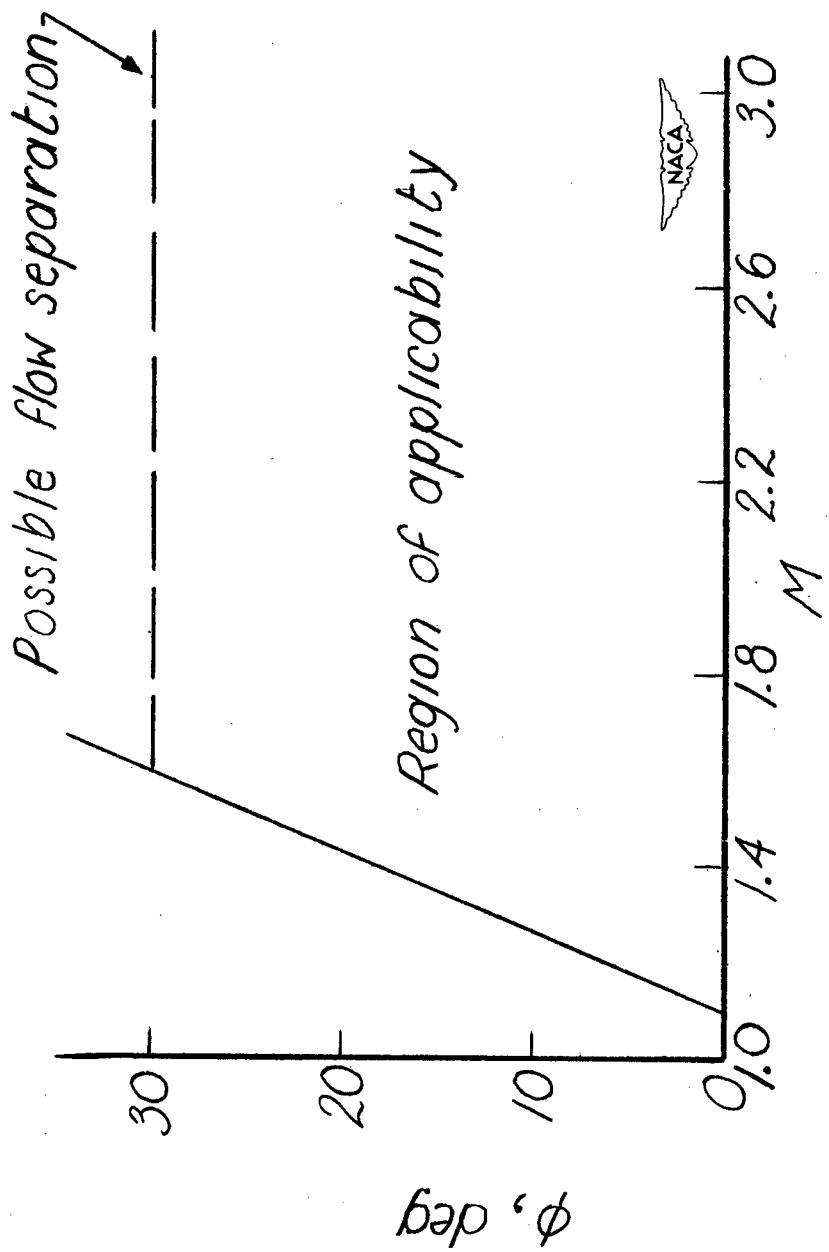
Figure 5.- Recommended region of applicability.